iScience

CellPress
OPEN ACCESS

Article

Single-cell transcriptional landscapes of bovine peri-implantation development

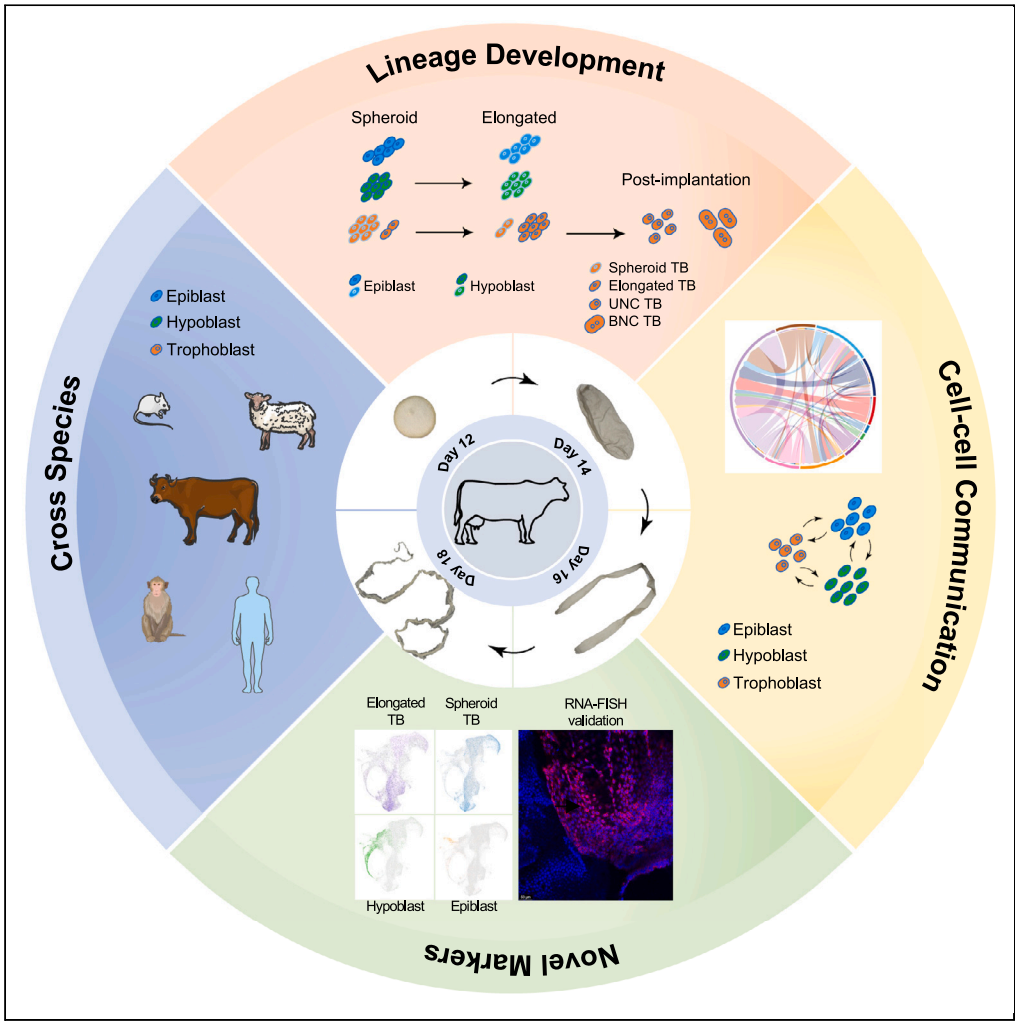

Giovanna Nascimento Scatolin, Hao Ming, Yinjuan Wang, ..., Chao Song, Kenneth Bondioli, Zongliang Jiang

z.jiang1@ufl.edu

Highlights

ScRNAseq analysis of peri-implantation reveals an unrecognized primitive trophoblast

Peri-implantation cell programs between bovine and other mammalian species are compared

Novel lineage markers are identified and validated

Cell-cell communication underlies embryonic and extraembryonic cell interaction

Scatolin et al., iScience 27, 109605
April 19, 2024
https://doi.org/10.1016/j.isci.2024.109605

iScience

CellPress
OPEN ACCESS

Article

Single-cell transcriptional landscapes of bovine peri-implantation development

Giovanna Nascimento Scatolin,[1,4] Hao Ming,[1,4] Yinjuan Wang,[2,3] Rajan Iyyappan,[1] Emilio Gutierrez-Castillo,[2] Linkai Zhu,[1] Masroor Sagheer,[1] Chao Song,[1] Kenneth Bondioli,[2] and Zongliang Jiang[1,5,*]

SUMMARY

Supporting healthy pregnancy outcomes requires a comprehensive understanding of the molecular and cellular programs of peri-implantation development, when most pregnancy failure occurs. Here, we present single-cell transcriptomes of bovine peri-implantation embryo development at day 12, 14, 16, and 18 post-fertilization. We defined the cellular composition and gene expression of embryonic disc, hypoblast, and trophoblast lineages in bovine peri-implantation embryos, and identified markers and pathway signaling that represent distinct stages of bovine peri-implantation lineages; the expression of selected markers was validated in peri-implantation embryos. Using detailed time-course transcriptomic analyses, we revealed a previously unrecognized primitive trophoblast cell lineage. We also characterized conserved and divergence peri-implantation lineage programs between bovine and other mammalian species. Finally, we established cell-cell communication signaling underlies embryonic and extraembryonic cell interaction to ensure proper early development. These data provide foundational information to discover essential biological signaling underpinning bovine peri-implantation development.

INTRODUCTION

Peri-implantation embryo development of ruminant species such as cattle is poorly understood and not closely paralleled to other animal models, such as the mouse. It is estimated that up to 50% of bovine conceptus loss occurs during the second and third weeks of pregnancy,[1,2] a period when a viable blastocyst undergoes extensive cellular proliferation and changes from a spherical shape to an elongated, filamentous form in preparation for implantation.[3] During this period, three cellular lineages form in the hatched bovine blastocyst, epiblast, hypoblast, and trophectoderm. As seen in all mammalian species, these lineages will give rise to the embryonic disc, which further develops into three germ layers, the yolk sac, and the placenta, respectively. At the molecular level, this critical stage of development has only been characterized in the mouse,[4,5] and more recently in non-human primates,[6] and human embryo extended culture models.[7,8]

Peri-implantation development exhibits wide variation between mammalian species in relation to the duration of peri-attachment periods, the development and orientation of the extraembryonic tissues, and the implantation strategies.[9] In mice, implantation occurs soon after blastocyst hatching from the zona pellucida. Within only a few days, it extends from implantation to placentation, where several dramatic and concurrent events occur, making it difficult to study the molecular and cellular changes during this time period in rodents. Studying peri-implantation development in humans is also problematic as embryos embed into maternal tissues after the blastocyst stage, and ethical issues limit the scope of possible research. However, in ruminants, such as cattle, the attachment of blastocysts is preceded by a period of rapid growth and elongation. This peri-implantation period is prolonged compared to rodents and is similar to that seen with human embryos. In this regard, the bovine is recognized as a highly informative model for human embryo development.[10–13]

However, the cell types in the developing peri-implantation embryo and molecular mechanisms governing the embryo elongation in ruminants remain unexplored. To fill this knowledge gap, we collected bovine embryos at day 12, 14, 16, and 18, and established a comprehensive single-cell transcriptomic landscapes of peri-implantation development. Using bioinformatics analyses, we define the development of three major cell lineages (trophoblast, hypoblast, and embryonic disc) and their gene expression dynamics throughout peri-implantation development. Together with a comparative analysis of bovine peri-implantation trophoblasts and mature placental trophoblasts,[14] we define and present a previously undefined trophoblast lineage. We also analyze cell-cell interaction signaling underling embryonic and extraembryonic cells interaction to ensure proper early development. This foundational information is useful to advance future efforts to understanding peri-implantation biology and causes of early pregnancy failure in the cattle.

[1]Department of Animal Sciences, Genetics Institute, University of Florida, Gainesville, FL 32610, USA
[2]School of Animal Sciences, AgCenter, Louisiana State University, Baton Rouge, LA 70803, USA
[3]Present address: Breeding and Reproduction of the Ministry of Agriculture and Rural Affairs, National Engineering Laboratory for Animal Science and Technology, China Agricultural University, Beijing, 100193, P.R. China
[4]These authors contributed equally
[5]Lead contact
*Correspondence: z.jiang1@ufl.edu
https://doi.org/10.1016/j.isci.2024.109605

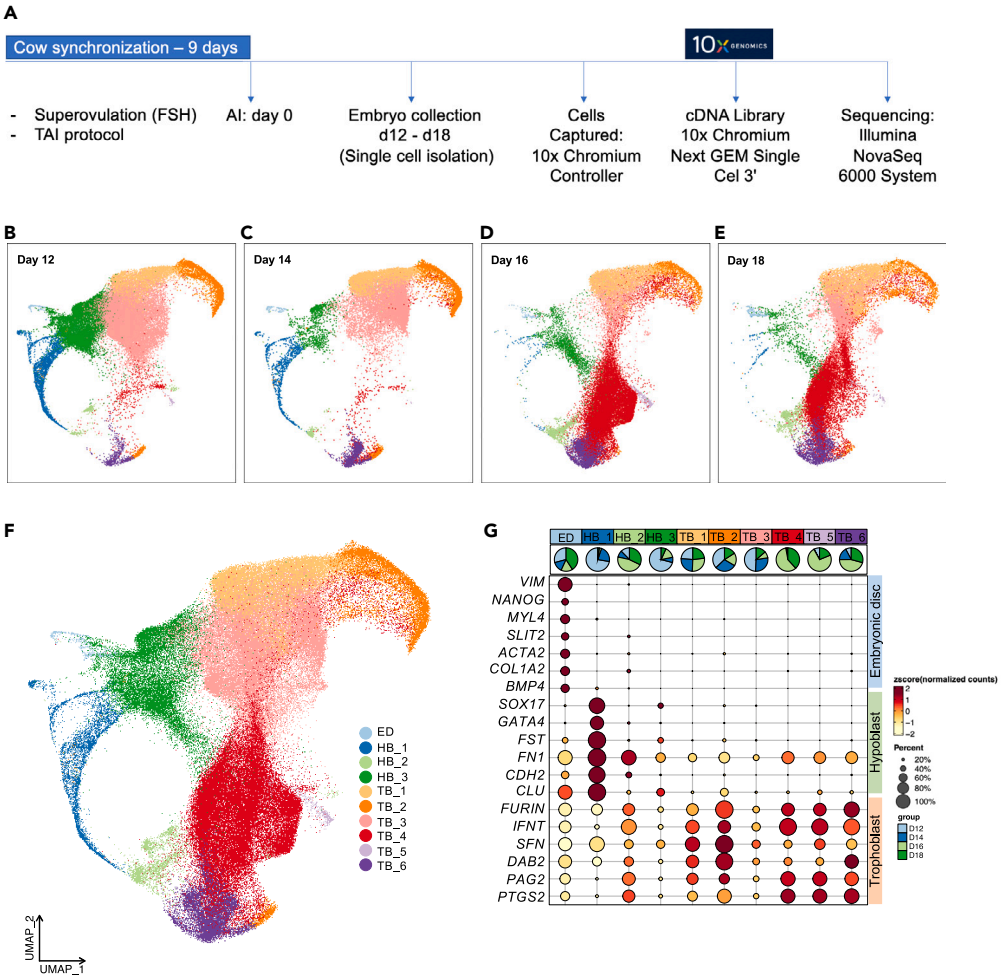

Figure 1. Single-cell RNA-seq (scRNA-seq) analysis of bovine peri-implantation embryo development

(A) Diagram of cow synchronization protocol, embryo collection and single-cell isolation and scRNA-seq procedures with 10x genomics approaches.

(B–E) Joint uniform manifold and projection (UMAP) analysis of transcriptomes of cell lineages from bovine peri-implantation embryos at day 12 (B), 14 (C), 16 (D), and 18 (E), and dynamic lineage developmental progress observed from day 12 through day 18.

(F) UMAP of integrated samples revealing 10 distinct cell types identified as embryonic disc (ED), hypoblast (HB) and different types of trophoblast (TB) cells.

(G) Dot plot representing the expression of gene markers for ED, HB, and TB development. Dot size represents the percentage of cells in the cluster expressing the gene markers, the color gradient represents the level of expression from high (red) to low (yellow) and pie chart represents the developmental stages presented in the cluster.

RESULTS

Construction of a single-cell transcriptomic census during bovine peri-implantation embryo development

To identify cell types and trajectories that lay the foundation for understanding bovine peri-implantation development, we performed single-cell RNA sequencing (scRNA-seq) using the 10X Genomics Chromium platform (Figure 1A). We sequenced mRNAs of individual cells from bovine peri-implantation embryos at day 12 (pooled ten day 12 embryos to increase the cell population), 14, 16, and 18 with biological replicates (Figures S1A–S1D). A total of 139,174 single cells from all peri-implantation stages were analyzed (Table S1). Joint uniform manifold and projection (UMAPs) and clustering analysis revealed ten distinct cell clusters for all cells within each developmental stage (Figures 1B–1E and S1E–S1H). To annotate the identities of cell clusters, we analyzed the database of known cell lineage markers in bovine,[15–19] humans and mouse,[20–22] and selected the markers that were detected in our single-cell transcriptomes of bovine peri-implantation embryos (Data S1). We identified *VIM, NANOG, MLY4, SLIT2, ACTA2, COL1A2,* and *BMP4* as marker genes of embryonic disc (ED), *SOX17, GATA4, FST, FN1, CDH2* and *CLU* as marker genes of hypoblast (HB), and *FURIN, IFNT, SFN, DAB2, PAG2* and *PTGS2* as trophoblast cell markers (Figure 1G). Using these markers, we captured three apparent major cell types in all four developmental stages, with 609 cells as ED, 21,283 cells as HB, and 117,282 cells as TB cell lineages (Figures 1B–1E and S1E–S1H; Table S1). Clustering analysis further revealed three subtypes of hypoblast cells and six subtypes of trophoblast cells (Figure 1F). As expected, the majority of cells analyzed were trophoblast cells due to the dramatic

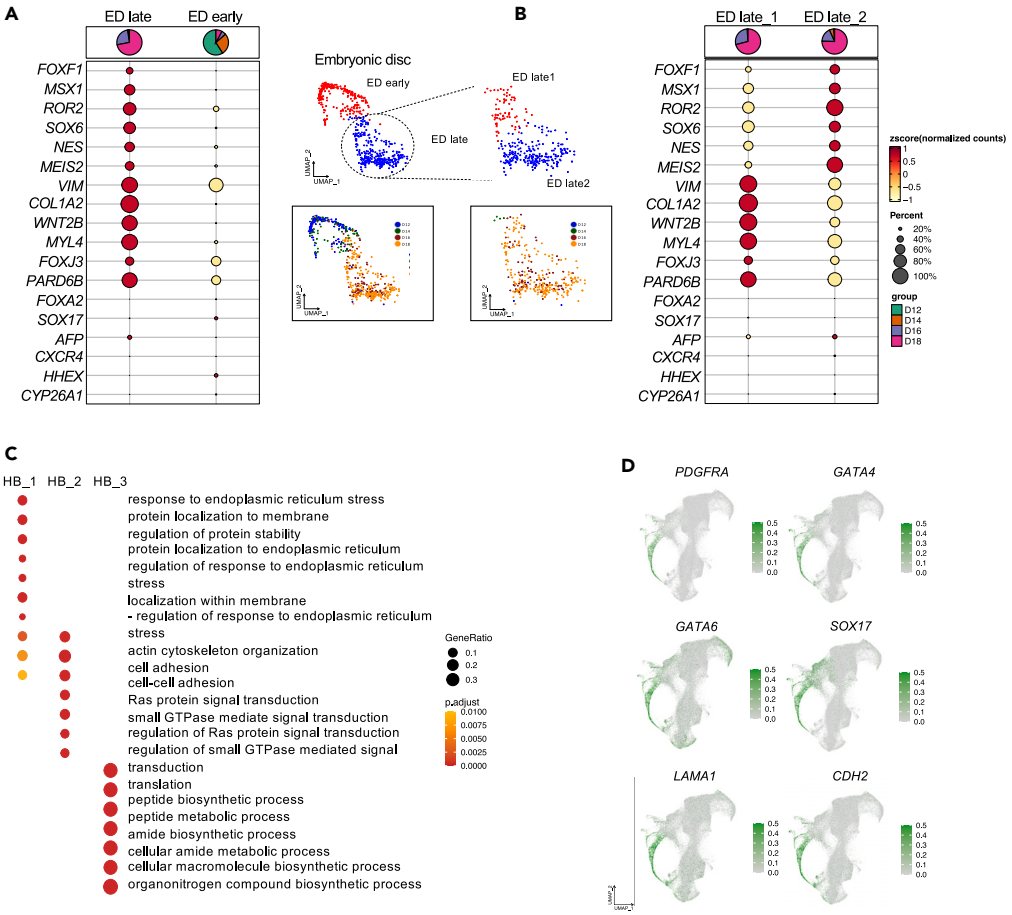

Figure 2. Identification of embryonic disc, germ layers and hypoblast lineages during embryo elongation

(A) Dotplot (left panel) and clustering (right panel) analysis of embryonic disc (ED) cell lineages. Two sub-clusters of ED were revealed (ED early and ED late). Highlighted area in blue were cells exclusively from day 16 and 18 (ED late) and red area with cells from day 12 and 14 (ED early). ED late highly expressed mesoderm and ectoderm markers (red dots).

(B) Re-clustering analysis of ED late cell lineages. Two additional sub cell types were revealed (ED late_1 and 2). Dotplot analysis of the expression of markers for ectoderm, mesoderm, and endoderm in the ED late_1 and 2 cells. Dot size represents the percentage of cells in the cluster expressing the gene, and the color gradient represents the level of expression from high (red) to low (yellow) and pie chart represents the developmental stages presented in the cluster.

(C) Dotplot showing the most represented GOs of genes specifically expressed in each of the hypoblast sub-lineages.

(D) UMAPs show the expression levels of common hyhoblast markers (*PDGFRA, GATA4, GATA6, SOX17, LAMA1, and CDH2)* among hypoblast clusters. The color gradient from gray to green at the right refers to the gene expression level (high expression = green).

trophectoderm (TE) elongation during bovine peri-implantation development. We found a clearly developmental progression of cell lineage transition, particularly trophoblast cell development as evidenced by alternations of cell clusters between early (day 12 and 14) and later (day 16 and 18) peri-implantation stages (Figures 1B–1E).

Development of embryonic disc during bovine peri-implantation development

Embryonic disc (ED) development is one of the major events during bovine conceptus elongation.[23] After epiblast and hypoblast segregation in the inner cell mass (ICM) at day 9 post-fertilization, the epiblast lineage further differentiates and forms the ED, which will contribute to the fetus after implantation.[24] We firstly clustered all cell populations merged from day 12 to day 18, ED cells were clustered into two sub-clusters that were clearly separated in UMAP (Figure 2A, top on the right panel). Group of cells in the cluster marked as blue were exclusively from day 16 and day 18 embryos (ED late), while cells in the other cluster (red) were from day 12 and day 14 embryos (ED early) (Figure 2A, bottom on the right panel). By further investigating the expression patterns of three germ layer markers (endoderm: *FOXA2, SOX17, AFP, CXCR, HHEX, CYP26A1,*[16,25] mesoderm: *FOXF1, MSX1, ROR2, SOX6, NES, MEIS,*[16,26] and ectoderm: *VIM, COL1A2, WNT2B, MYL4, FOXJ3, and PARD6DB,*[27,28] only cells in the ED late cluster showed the anticipated increase of those marker genes except for common endoderm markers, indicating mesoderm and ectoderm form by embryonic day 16 in bovine (Figure 2A, left panel). To explore the initiation of germ layer

development, we performed clustering analysis only on the cells belonging to the embryonic germ layers (ED late, Figure 2B, left panel). These cells were further divided into two new sub-clusters (ED late_1 and ED late_2), which highly expressed mesoderm and ectoderm markers, respectively (Figure 2B, right panel). Together, these results indicate that germ layer development starts from day 16 after fertilization in bovine, with the formation and segregation of mesoderm and ectoderm lineages first, followed by the endoderm layer which arises after day 18.

Development of hypoblast during bovine peri-implantation development

Primitive endoderm (PE) or hypoblast (HB), which gives rise to the yolk sac after implantation, is critical to support early conceptus development.[29] We next characterized hypoblast development during bovine peri-implantation development. Three subtypes of hypoblast were identified and showed distinct characteristics, 1) the majority of hypoblast cells were the HB_1 subtype in embryos at day 12 and 14 (blue, Figures 1B–1E), HB_2 cells were present across all stages with increased cell populations during development from day 12–18 (light green, Figures 1B–1E), on the contrary, HB_3 cells had decreased populations from day 12 to day 18 and clustered more closely to HB_2 cells as development progresses (dark green, Figures 1B–1E); 2) functional gene ontology (GO) analysis of the highly expressed genes in each of the hypoblast cell subtypes revealed a significant enrichment in the expression of genes related to response to endoplasmic reticulum stress, protein localization to membrane, regulation of protein stability in HB_1 cells, actin cytoskeleton organization, cell adhesion, ras protein signal transduction in HB_2 cells, and finally translation, biosynthetic process, and metabolic process in HB_3 cells (Figure 2C); 3) well known hypoblast lineage markers showed unique patterns between the subtypes, i.e., HB_1 cells were marked by *PDGFRA* and *GATA4*, HB_1 and 3 were positive for *GATA6* and *SOX17*, and *LAMA1* and *CDH2* were enriched in HB_1 and 2 cells (Figures 2D and S2A). This is consistent with the notion that these lineage markers contribute to conserved hypoblast lineage segregation in different mammalian species[17,30]; 4) we characterized the developmental progression of the three hypoblast subtypes by trajectory analysis and found they are originated as HB_1, and progressed toward HB_3 and HB_2 (Figure S2B). The presence of HB_1 and 3 during early stages followed by HB_2 present at later stages, suggests a coordinated development of hypoblast lineages during bovine early development.

Dynamics of trophoblast lineage development during bovine peri-implantation development

Trophectoderm (TE) elongation is an unique process in ruminants, during which undifferentiated TE cells, or trophoblast progenitor cells will differentiate to mononucleated or uninucleate trophoblast cells (UNC) to drive embryo elongation and secrete interferon tau (IFNT), a signal for maternal fetal recognition.[31,32] A subset will subsequently differentiate into binucleate cells (BNC)[33,34] in preparation for attachment with the maternal endometrium. Many studies have provided abundant data concerning the TE of blastocysts[17,18] or trophoblasts after placentation,[34] however, the trophoblast cell fate during the bovine peri-implantation period remains poorly understood. Using 14 widely accepted marker genes for bovine trophoblast cell lineages,[16,35] we were able to classify six trophoblast subtypes into two major lineages during bovine peri-implantation development (Figures 1B–1G, 3A, and 3B). The first with proliferative potential highly expressing *ASCL2, CDX2, and RAB25* and mainly present in spheroid embryos at day 12 and 14, and thus were defined as spheroid TB (TB_1, 2, and 3). A second subtype with the increased expression of trophoblast markers including *IFNT*, *PTGS2*, and *SSLP1* but not binucleate cell markers, were specifically enriched in elongated embryos at day 16 and 18, and therefore were deemed as elongated TB (TB_4, 5, and 6) (Figures 1B–1G, 3A, and 3B). This analysis suggests that this newly identified primitive trophoblast cells (elongated TB) are responsible for pregnancy maintenance in bovine prior to the time when binucleate cells emerges. Our immunostaining analysis further confirmed the presence of ED marker *VIM* and TB marker *KRT8*, *PTGS2* (Figures S2C and S2D). The immunostaining analysis confirmed the absence of BNCs in peri-implantation embryos from days 12–18 by staining with f-actin (Figure S2E), which is consistent with the previous observation that BNC begins to appear on day 20 of pregnancy.[33,34] During trophoblast development, trophoblast lineage composition on days 12 and 14 were similar but distinct from those at days 16 and 18, demonstrating a marked shift of trophoblast lineage composition from spheroid embryos in days 12 and 14 to elongated embryos in days 16 and 18 (Figures 1B–1E). This was further confirmed by the pseudotime trajectory analysis showing trophoblast development starts with TB_1, 2, 3 (spheroid TB that are toward to the right edge of the tree) and progresses toward TB_4, 5, 6 (elongated TB enriched on the left edge of the tree) (Figure 3C).

To understand the biological function of trophoblast sub-lineages during bovine elongation, we first analyzed the trophoblast stage-specific genes that corresponded to different peri-implantation stages (Figure 3D). Interestingly, analysis of the functions of these stage-specific genes revealed a sequential progression of trophoblast stage-specific core gene networks. It migrated from peptide metabolic processes, translation, and biosynthetic processes in day 12, to the regulation of translation, metabolic processes and mitochondrial function in day 14, to actin cytoskeleton organization, cell adhesion, and fatty acid metabolism processes in day 16, and finally to the regulation of embryonic development, epithelium, tube, tissue, blood vessel and vasculature development in day 18 (Figure 3D). Such coordinated changes of functional pathways further confirmed trophoblast cell development transitions from spheroid to elongated TB cells and are reflective of the general lack of knowledge concerning trophoblast lineage identities and gene expression patterns during this critical period of development in cattle. Second, we explored the specific genes with enriched expression in the transition of the two major trophoblast lineages. It was found that several trophoblast gene markers and genes related to ribosome activity were highly expressed in spheroid TB including *KRT8, KRT18, PLAC8A, H2AZ*, and RPL (Ribosomal Protein Large) subunit gene family (Figure 3E). However, genes highly expressed in elongated TB including *BCAR3*,[36] *FGD4*,[37] and *PLEKHA5*[38] (Figure 3E), suggesting that elongated TB might be critical for the elongation process, embryo attachment, and implantation.[9,34] Third, we analyzed the cell cycle composition of separate trophoblast clusters and found a higher proliferative status in elongated TB cells (Figure 3F). Finally, a list of highly expressed genes was identified in a trophoblast cell subtype-specific

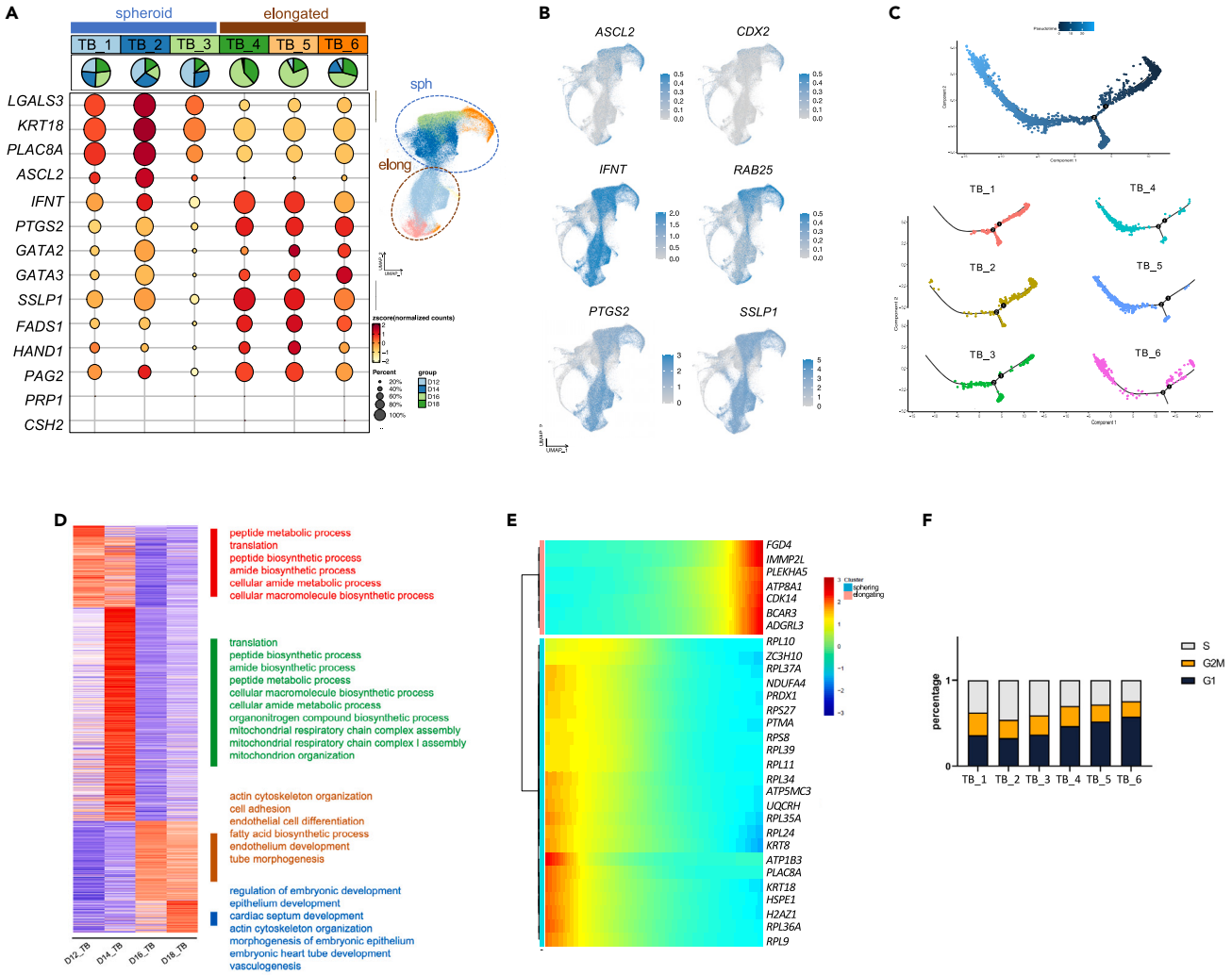

Figure 3. Dynamics of trophoblast lineage development in bovine peri-implantation embryos

(A) Dotplot (left panel) presenting common trophoblast markers in the trophoblast clusters and classification of spheroid and elongated cells. Dot size represents the percentage of cells in the cluster expressing the gene, and the color gradient represents the level of expression from high (red) to low (yellow) and pie chart represents the developmental stages presented in the cluster. On the right panel, trophoblast cell lineages of spheroid embryos (blue circle represents TB_1, 2, and 3) and elongated embryos (brown circle represents TB_4, 5, and 6) were divided by UMAP analysis.

(B) UMAPs showing the expression levels of *ASCL2, CDX2, RAB25, IFNT, PTGS2, and SSLP1* (common trophoblast markers). *ASCL2, CDX2, and RAB25* were highly expressed in trophoblast cells from spheroid embryos; *IFNT, PTGS2,* and *SSLP1* were highly expressed in trophoblast cells from elongated embryos.

(C) Pseudotime analysis of trophoblast lineage development. Top panel: Two start points of development were identified in the right edge by dark blue. Bottom panel: the distribution of clusters demonstrated the development of TB_1, 2, and 3 (spheroid) into TB_4, 5, and 6 (elongated).

(D) Heatmap showing top enriched pathways from genes specifically expressed in each developmental stage of trophoblasts.

(E) Heatmap shows the scaled expression of dynamic genes along Pseudotime of trophoblast development between spheroid TBs at left side and elongated TBs at right side. The color bar represents the *Z* score distribution from −3 (blue) to 3 (red).

(F) Cell cycle composition (S, G2/M, and G1 phases) of TB clusters.

manner (Figure S2F). The genes with the most dynamic changes during trophoblast development included *ADAMTS1, AHSG, ATP5PO, CSTB, FETUB, LPP, PTTG1IP,* and *TP63* (Figure S2G), implying their essential roles in manipulating trophoblast differentiation during this period.

Trophoblast lineage development and differentiation from day 12 to day 195 of pregnancy in cattle

By integrating peri-implantation trophoblast cell lineages with the recently two published single-cell transcriptomes of trophoblasts from day 17 through day 195 of pregnancy in cattle,[14,39] we constructed a comprehensive transcriptomic road map of trophoblast lineage development

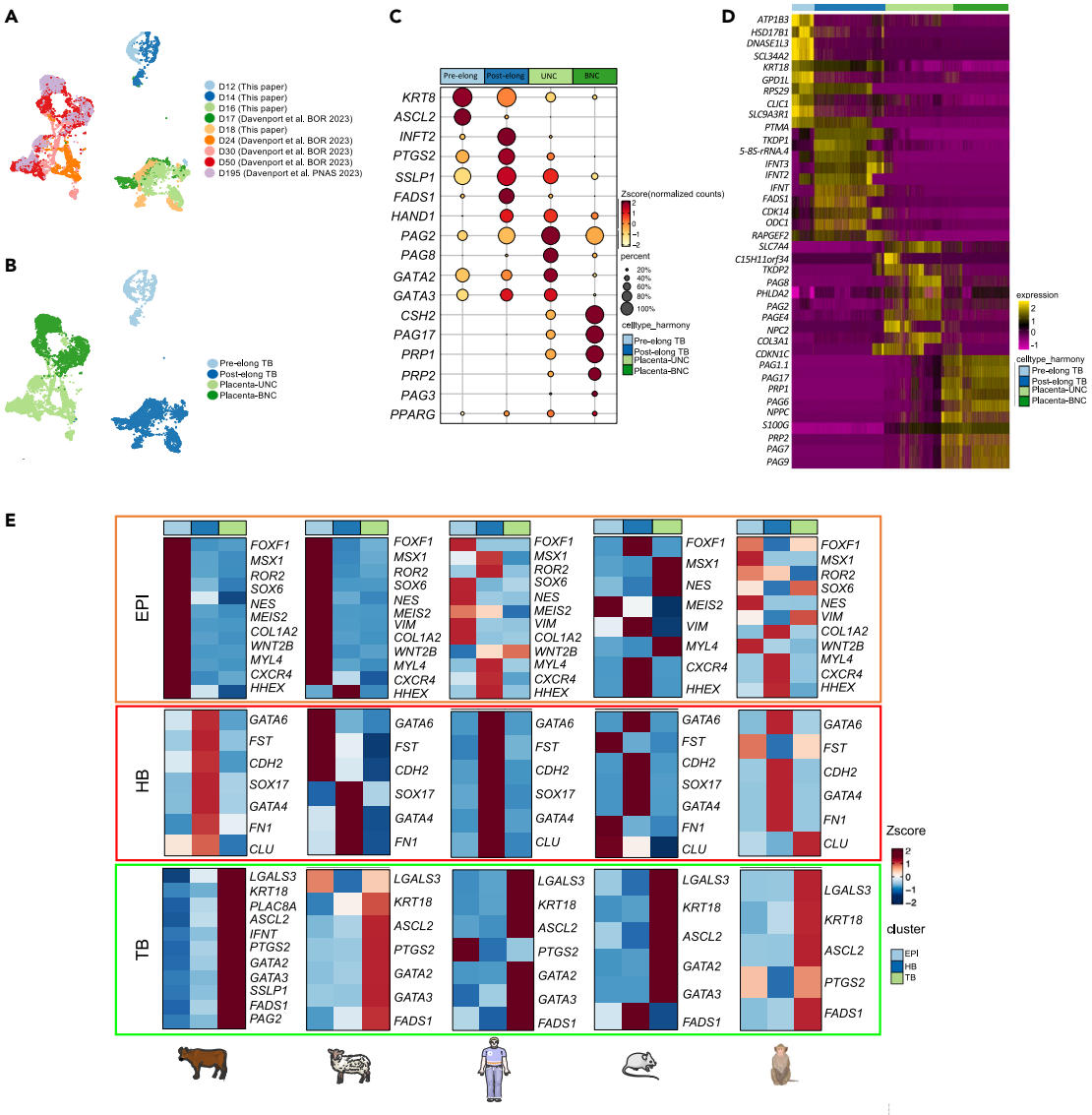
A
D12 (This paper)
D14 (This paper)
D16 (This paper)
D17 (Davenport et al. BOR 2023)
D18 (This paper)
D24 (Davenport et al. BOR 2023)
D30 (Davenport et al. BOR 2023)
D50 (Davenport et al. BOR 2023)
D195 (Davenport et al. PNAS 2023)
B
Pre-elong TB
Post-elong TB
Placenta-UNC
Placenta-BNC
C
Pre-elong
Post-elong
UNC
BNC
KRT8
ASCL2
INFT2
PTGS2
SSLP1
FADS1
HAND1
PAG2
PAG8
GATA2
GATA3
CSH2
PAG17
PRP1
PRP2
PAG3
PPARG
Zscore(normalized counts)
percent
celltype_harmony
Pre-elong TB
Post-elong TB
Placenta-UNC
Placenta-BNC
D
ATP1B3
HSD17B1
DNASE1L3
SCL34A2
KRT18
GPD1L
RPS29
CLIC1
SLC9A3R1
PTMA
TKDP1
5-8S-rRNA.4
IFNT3
IFNT2
IFNT
FADS1
CDK14
ODC1
RAPGEF2
SLC7A4
C15H11orf34
TKDP2
PAG9
PHLDA2
PAG2
PAGE4
NPC2
COL3A1
CDKN1C
PAG1.1
PAG17
PRP1
PAG6
NPPC
S100G
PRP2
PAG7
PAG9
expression
celltype_harmony
Pre-elong TB
Post-elong TB
Placenta-UNC
Placenta-BNC
E
EPI
HB
TB
FOXF1
MSX1
ROR2
SOX6
NES
MEIS2
VIM
COL1A2
WNT2B
MYL4
CXCR4
HHEX
GATA6
FST
CDH2
SOX17
GATA4
FN1
CLU
LGALS3
KRT18
PLAC8A
ASCL2
IFNT
PTGS2
GATA2
GATA3
SSLP1
FADS1
PAG2
Zscore
cluster
EPI
HB
TB
F
Bovine
Human
ANLN
EPCAM
CALM2
CDX2
CSH2
LGALS1
spheroid TB
elongated TB
UNC TB
BNC TB
CTB
STB
EVT
G
Bovine
Human
translation
peptide biosynthetic process
cellular macromolecule biosynthetic process
mitochondria organization
cellular respiration
generation of precursor metabolites and energy
regulation of translational initiation
small molecule biosynthetic process
actin filament -based process
actin cytoskeleton organization
cytoskeleton organization
regulation of DNA-templated transcription
cell migration
negative regulation of biosynthetic process
cell-cell junction assembly
protein target to ER
regulation of cell projection assembly
actin filament polymerization
autophagy
establishment of protein localization
Sphe TB
elong TB
UNC TB
BNC TB
CTB
EVT
STB
p.adjust
GeneRatio

Figure 4. Comparative analysis of trophoblast cell lineage development during bovine pregnancy and across mammalian species

(A and B) Integrated analysis of single-cell transcriptomes of trophoblast lineage cells from different stages of developing bovine embryos (D12, 14, 16, 17, 18) and day, 24, 30, 50 and 195 placentas.

(C) Dotplot shows the expression levels of trophoblast markers. Dot size represents the percentage of cells in the cluster expressing the gene, and the color gradient from red to yellow represents the level of expression from high to low.

(D) Heatmap of the top marker gene list for four trophoblast lineages.

(E) Heatmap of the expression levels of common lineage markers during peri-implantation development across five mammalian species.

(F) Violin plot comparing common TB markers in bovine and human peri-implantation development.

(G) Dotplot comparison of representative biological functions between TB lineages of human (CTB, STB, and EVT) and bovine (spheroid TB, elongated TB, UNC, and BNC). Color from light blue to red represents the p value from high to low, and size from small to large represents gene ratio from low to high.

and differentiation. Clustering analysis classified trophoblast lineages into three major groups based on the development stage (cluster 1: day 12–14; cluster 2: day 16–18; cluster 3: day 24–195 (Figure 4A). It is notable that day 17 trophoblasts from the published dataset were grouped well with those of day 16 and 18 from this study (Figure 4A), indicating the reliability of the integrate analysis. Based on the morphology and function, we could further classified them into four trophoblast groups during bovine pregnancy (Figure 4B), i.e., 1) pre-elongated TB mostly regarded as spheroid TB from day 12–14 embryos, 2) post-elongated TB from a mixture spheroid and elongated TB in day 16–18 embryos, 3) placenta-UNC TB from day 24 to day 195 placenta, and 4) placenta-BNC TB that are exclusively from day 30 placenta and beyond.

Interestingly, we found that common trophoblast markers had a coordinated expression along trophoblast development and differentiation. For example, the expression of pre-elongated TB markers including *KRT8* and *ASCL2* were gradually decreased from pre-elongated TB to BNC (Figure 4C). The expression of *INFT2, PTGS2,* and *FADS1* emerged in pre-elongated TB, then peaked in post-elongated TB, and finally decreased dramatically in UNC and BNC after implantation, while other genes such as *SSLP1* and *HAND1* stayed active in UNC after implantation (Figure 4C). On the contrary, BNC markers including *CSH2, PAG17,* and *PRP1/2/3* were exclusively expressed in post-implantation TB (Figure 4C). In addition, trajectory analysis predicted two separate differential routes, the first from pre-elongated TB (day 12/14) to post-elongated TB (day 16/17/18), the second from placenta UNC emerging right after attachment (day 24/30) to BNC of more matured placentas (day 30/50/195) (Figure S3A). The gap between the two trajectories indicates that TB experience dramatic differentiation processes during implantation. Again, analysis of the functions of the highly specifically expressed genes from each of the four identified trophoblast types reflected their sequential progression of trophoblast differentiation programs during bovine pregnancy (Figure S3B).

Comparative analysis of lineage development in mammalian peri-implantation embryos

To reveal the conserved and divergent programs of lineage development across mammalian species, we conducted comparative analysis of single-cell transcriptomic profiles of peri-implantation embryo development from mouse,[40] human,[41] sheep,[42] and monkey.[43] Overall, clustering analysis showed that the three main lineages (HB, EPI, and TB) were nicely clustered together regardless of species (Figure S3C), indicating the conservation of lineage development programs during peri-implantation development. We then analyzed the common genes shared between bovine and other species among the three main lineages (Figure S3D). We found EPI has the largest number of common genes shared between bovine and other species compared to HB and TB (Figure S3D, left panel). GO analysis of the shared genes revealed common gene networks that are regulating key processes during embryo development, such as gastrulation, stem cell population maintenance, and cell communication in EPI; angiogenesis, epithelium development, and lipid transport in HB; as well as embryonic morphogenesis, cytoskeleton organization, and reproductive system development in TB (Figure S3D, right panel). The two ruminant species analyzed, bovine and sheep shared similar lineage development programs as expected (Figure S3D).

We then analyzed the expression of lineage markers that are shared among five mammalian species (Figure 4E). Most of EPI and TB lineage marker genes in bovine were highly expressed in corresponding lineages of sheep except for *HHEX,* which is an EPI marker in bovine but an HB marker in sheep (Figure 4E). On the contrary, the HB markers showed vast inconsistency between sheep and bovine, e.g., bovine *GATA6, FST*, and *CDH2* were presented as sheep EPI markers (Figure 4E). Intriguingly, bovine and human shared all identified HB and TB lineage markers, except for *PTGS2* being enriched in EPI in both human and monkey (Figure 4E). The bovine EPI markers were either enriched in EPI or HB in humans, except for *WNT2B* (Figure 4E). Marker genes analysis also suggested mouse has the most divergent lineage marker gene expression compared with all other mammalian species (Figures 4E and S3D).

Since our analysis indicates the potential value of using cow as a model for studying human peri-implantation development, we further explored the trophoblast lineage development programs between bovine and human. In this analysis, we focused on our identified bovine trophoblast lineages and compared them to human cytotrophoblast (CTB), syncytiotrophoblast (STB), and extravillous trophoblast (EVT). We found that human CTB markers including *ANLN, EPCAM, CALM2,* and *CDX2*, were enriched in bovine pre-elongated TB, and EVT markers *CSH2* and *LGALS1* were highly expressed in bovine placenta UNC and BNC (Figure 4F). On the contrary, human STB markers were not enriched in bovine trophoblast in a specific lineage manner (Figure 4F), suggesting different functionality of STB and BNC in their corresponding species despite being the same multinucleated cells. The functional analysis of lineage-specific genes further confirmed our observations that human CTB resembles bovine pre-elongated TB as both are being pluripotency proliferating trophoblasts (Figure 4G). The other bovine TB cell types including placenta BNC, shared common gene networks with human EVT (Figure 4G), indicating that unlike human, the invasive, but not secretory properties are dominating multinucleated cells, placenta BNC in bovine. Our analysis provides new insights of conserved and divergent trophoblast lineage development programs between bovine and human.

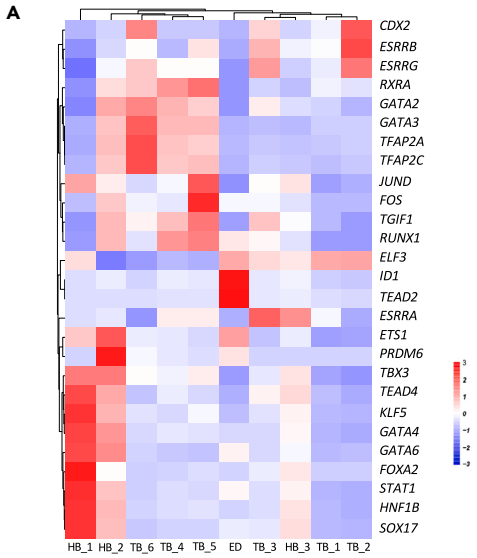

B

Bovine Novel Markers

Spheroid TB	Elongated TB	Hypoblast	Embryonic disc
TMEM86A	*RAPGEF2*	*CTSV*	*PLTP*
CFAP54	*RBM47*	*ADAMTS9*	*PTMA*
FXYD4	*PLEKHA5*	*RASGRF2*	*MS4A8*
PINLYP	*ADGRL3*	*RCN1*	*PSIP1*
SEC61G	*ERC2*	*SKAP1*	*CDC42EP5*
TOMM5	*RABPC1*	*SPINT2*	*PRTG*
NDUFB1	*PTTG1LP*	*CASK*	*RORA*
AMDHD2	*SATB2*	*FOXP1*	
C1QBP	*ASAP1*	*FHOD3*	
MANF	*KIF13B*	*RBFOX2*	

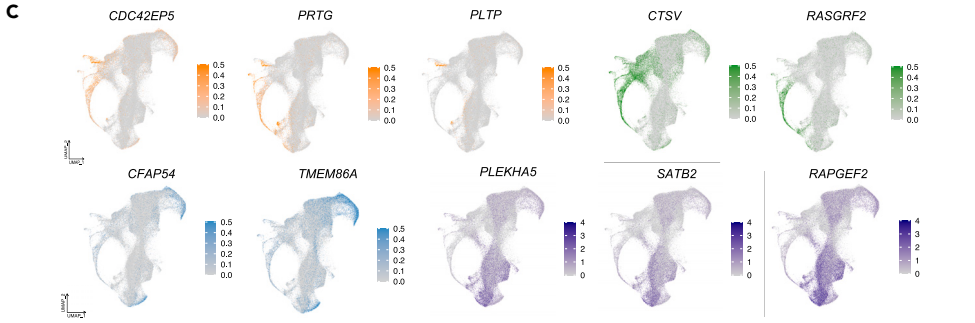

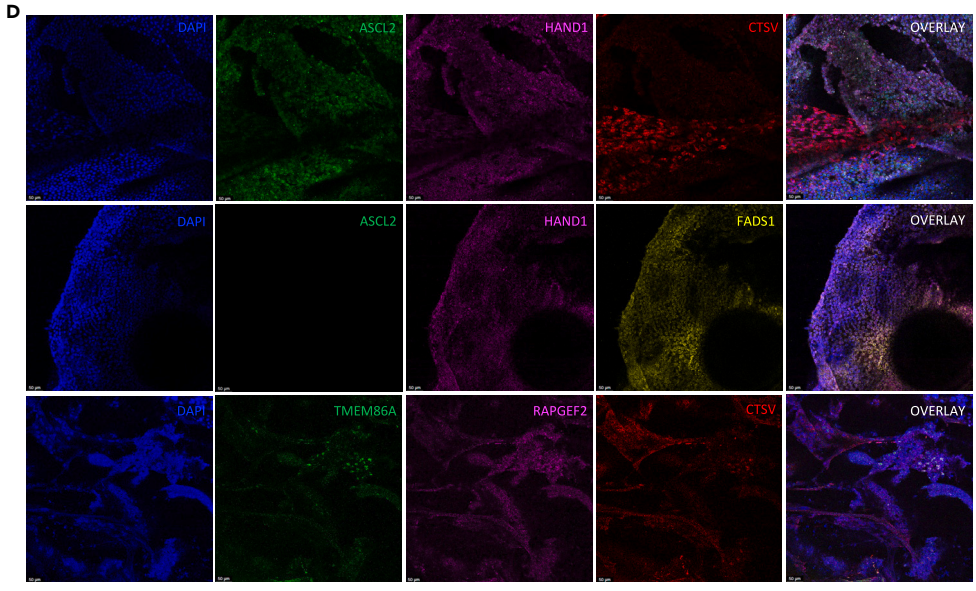

Figure 5. Identification of the transcriptional factors and novel lineage markers during bovine peri-implantation development

(A) Heatmap of transcription factors identified in bovine peri-implantation embryos. Each column represents a different lineage. The relative level is represented by the gradient color from blue to red.

(B) Table of identified novel gene markers for ED, HB, and TB.

(C) UMAPs showing the expression levels of identified novel makers in ED (orange), HB (green), spheroid TB (blue) and elongated TB cells (purple).

Figure 5. *Continued*

(D) Representative image of RNA-FISH analysis of day 14 and 16 embryos. Embryos hybridized with probes sets specific to *ASCL2*, *HAND1*, and *CTSV* in day 14 bovine embryos, *ASLC2, HAND1, FADS1, and CTSV* in day 16 bovine embryos, and *TMEM86A, RAPGEF2*, and *CTSV* in day 16 bovine embryos. The white scale bar for each image is 50 μm).

Identification of the transcriptional factors and novel lineage markers during bovine peri-implantation development

Given that most known transcriptional factors (TFs) are essential developmental regulators and are limited to pre-implantation embryos,[44,45] here we identified transcriptional factors (TFs) during bovine peri-implantation embryos and explored the key regulators directing the development of specific cell lineages (Figure 5A). For example, important mediators for trophoblast stem cell self-renewal (*CDX2, ESRRB, GATA2, GATA3, TFAP2A*, and *TFAP2C*),[46] epiblast development (*TEAD2*),[47] and primitive endoderm (*GATA4, GATA6, SOX17*, and *TBX3*)[48] were prioritized in the bovine peri-implantation development (Figure 5A). We also identified little known regulators for lineage specification including *PRDM6, TGIF1*, and *HNF1B* (Figure 5A).

Since most of the early cell lineages markers have been studied in mouse early development, we next sought to identify the novel markers in bovine early cell lineages (Figure 5B). First, we identified novel markers associated with identified ED (Figure 5C). The highly expressed genes specifically enriched in ED lineages included *CDC42EP5*, a regulator of cytoskeleton organization and migration,[49] *PRTG*, that is essential for mesoderm and nervous tissue development[50] and *PLTP*, a mediator of lipoprotein metabolism and transport[51] (Figure 5C). Second, we found *CTSV* and *RASGRF2* as novel markers for hypoblast cells (Figure 5C). Third, we investigated novel markers for trophoblast cell lineages and found that *CFAP54* and *TMEM86A* had a significant high expression in spheroid TB cells, while *PLEKHA5, SATB2*, and *RAPGEF2* marked elongated TB cells (Figure 5C). More importantly, we validated these novel markers during dynamic transition period of day 14 and day 16 bovine embryos using the RNA-FISH technique. We first conducted negative and positive controls (GAPDH) to validate the technique in the bovine embryos (Figure S4). We were able to validate the presence of spheroid TB markers (*ASCL2, TMEM86A*), elongated TB markers (*HAND1, FADS1*, and *RAPGEF2*), and HB marker (*CTSV*) in corresponding lineages (Figures 5D and S4). A more in-depth investigation into these novel markers has the potential to unveil new insights into their regulatory roles in bovine conceptus elongation, implantation, and placentation.

Embryonic and extraembryonic cell-cell interactions during bovine peri-implantation development

Faithful embryogenesis and success of pregnancy establishment require a precise coordination between embryonic and extraembryonic lineages.[52] Here we sought to identify the cell-cell interaction signaling between lineages contributing to embryonic and extraembryonic tissues in bovine. We explored the signaling interactions (Figure 6A) and identified ligand and receptor pairs (Figure 6B) among lineages using Cell Chat analysis (see STAR methods). Based on the number of signaling interactions from each lineage, we found that TB_1, 3 and HB_3 lineages work independently from other cells with less outgoing and incoming signaling (Figure 6B). Conversely, HB_1 was shown to be an interactive lineage, with the most sender and receiver signaling. Additionally, HB_1 received massive signals from TB_2 (spheroid TB) and sent most of the signals to TB_6 (elongated TB) (Figure 6B), suggesting that HB_1 could be an important mediator for trophoblast differentiation and thus promotes embryo elongation.

Of note, two well-known signaling pathways, WNT and IGF, were found to be outgoing signal in UNC (Figure 6C), and an outgoing signaling in ED (Figure 6D), respectively. It is noteworthy that IGF is essential for fetus development and growth,[53] while WNT signaling is a crucial factor affecting both embryonic and extraembryonic stem cell maintenance.[54,55] Additionally, we found ED was an important sender of MK and PTN signaling that have important functions in cell proliferation, migration, and self-renew.[56] Interestingly, both shared the same receptors (PTPRZ1 and SDC2/4) in both hypoblast and trophoblast lineages (Figures 6E and 6F), suggesting HB and ED mediate the development of extraembryonic lineage development.

Together, the identification of these cell-cell interaction molecules provides candidate regulators for further mechanistic studies underly how embryonic and extraembryonic cells interact to ensure proper early development in bovine.

DISCUSSION

Peri-implantation development is a critical period when most pregnancies fail yet is the least studied process during mammalian development. In the bovine, peri-implantation is defined by embryo elongation prior to attachment. During this process, the blastocyst cells proliferate massively, the initially un-limited potential of the epiblast is restricted and shaped by a combination of changes in cell lineage composition. Additionally, gene expression, cell-cell interactions, and physical forces - toward defined germ layers and cell types, as well as the trophoblast progenitors differentiating to form the primitive placenta and initiate maternal fetal recognition,[31,32] all work coordinately to establish the successfully pregnancy. Here, we have provided a single-cell transcriptomic wide characterization of these cellular and molecular events accompanying the bovine embryo elongation. The datasets, particularly when mined further and integrated with epigenome information, are expected to greatly expand our understanding of the gene regulation mechanisms governing bovine peri-implantation embryo development, which will provide valuable insight into what can potentially go wrong in the pregnancies that fail during this period.

Our study revealed the timing and cell types emerging in a coordinate fashion during bovine early development and observed some surprises. First, epiblast, later embryonic disc developed into mesoderm and ectoderm in embryo days 16 and 18 while the endoderm emerged much later. This is quite interesting as it is in contrast with the mouse, where the declining of epiblast cells is followed by mesoderm and endoderm lineage development and ectoderm development one day later.[57] Second, our analysis identified a previously unrecognized primitive

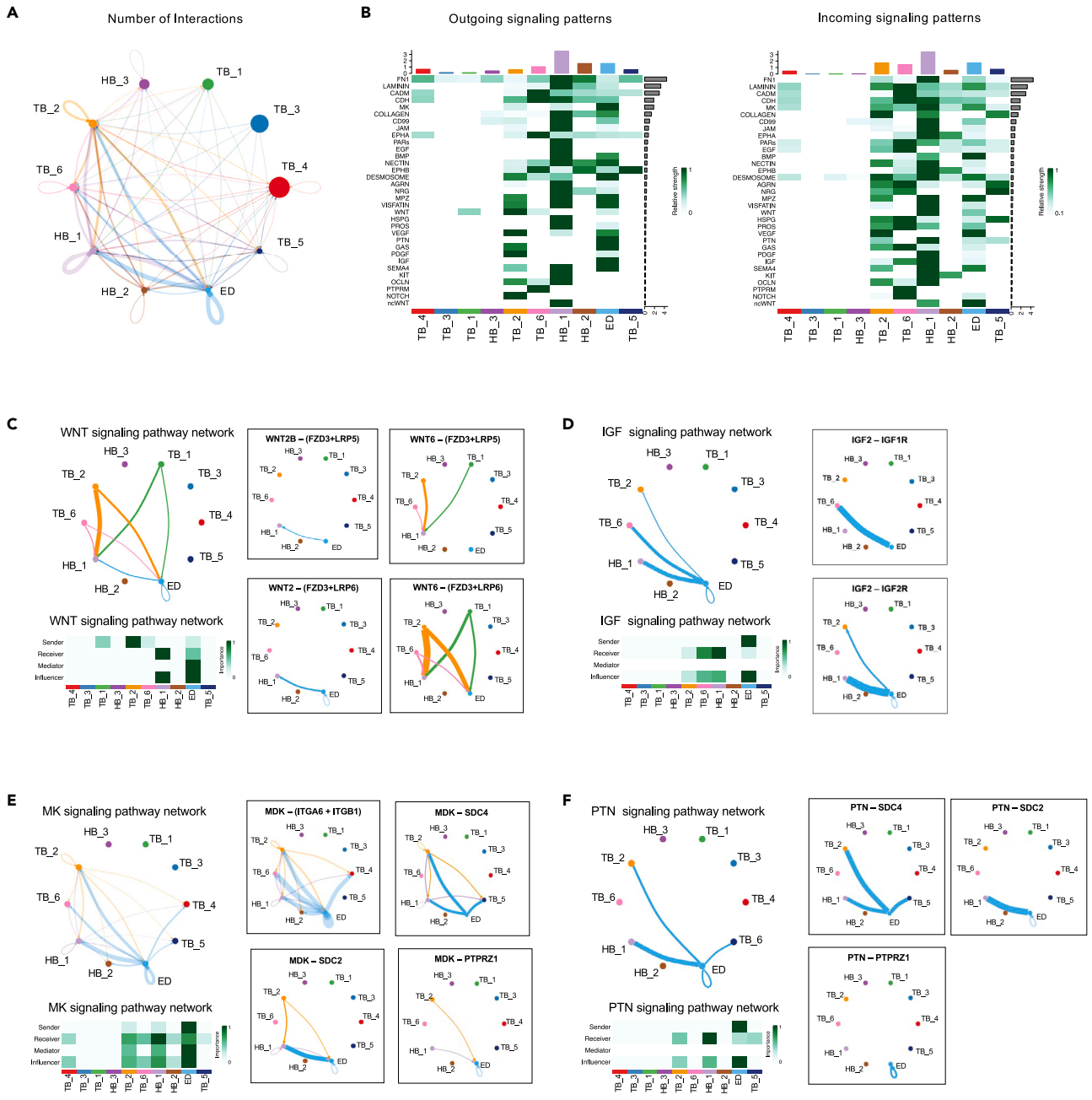

Figure 6. Embryonic and extraembryonic cell-cell interactions during bovine peri-implantation development

(A) Interaction analysis shows the significant cell–cell interaction among different cell lineages. Arrows and edge color indicate direction (ligand: receptor), the circle size represents the number of cells and edge thickness indicates the communication probability.

(B) Heatmap showing the identified pairs of ligand and receptor signaling in the embryonic and extra-embryonic cell lineages of bovine peri-implantation embryo. Outgoing signaling is presented on the left panel, and incoming signaling is presented on the right panel. The color gradient on the left represents the relative signaling strength of the signaling pathway across clusters.

(C–F) On the left panel, circle plot shows the intercellular communication network for WNT, IGF, MK and PTN signaling and heatmap showing the relative importance and contribution of each cell lineage to the overall communication network. On the right panel, circle plot shows the identified ligands and respective receptors in each signaling.

trophoblast cell lineage, termed as elongated TB and confirmed the absence of the binuclear cells by day 18 bovine embryos. Third, trophoblast cell development is very dynamic, trophoblast cells at days 12 and 14 appear spheroid, while a major shift occurs at day 16, when elongating cells become dominant. This dramatic change is also coordinate with the embryo's dramatic elongation in size from an elongated form

at day 14 to a filamentous form at day 16. Interestingly, the embryo changes from a spherical shape at day 12 to elongated form at day 14, however, day 12 and day 14 embryos have very similar cell composition and transcriptomes, suggesting that the bovine embryo elongation may not be driven by embryo internal genetic factors.

As expected, most of the cells analyzed in the bovine peri-implantation embryo are trophoblast cell lineages. In our dataset, we identified six different sub-lineages of trophoblast cells, classified into two categories as spheroid TB and elongated TB. By integrated analysis early trophoblast lineages with the published more advanced trophoblasts after implantation and placentation,[14,39] we further constructed a comprehensive transcriptomic road map of trophoblast lineage development and differentiation. While BNC cells are not present in the peri-implantation embryos, these newly identified elongated TB cells have up-regulated machinery for the BNC cells and represent an important stage of trophoblast cell fate that is responsible for pregnancy maintenance in bovine prior to the emergence of binucleate cells. The identification of these progressive functions is also the first step to reveal the importance of elongated TB cells in the formation of the functional placenta and maintenance of the pregnancy.

In addition, our comparative analysis revealed remarkable conserved and divergent programs between bovine and human trophoblast development. For example, bovine pre-elongated TB shares similarities with human CTB, being proliferative and related to metabolic process and mitochondria organization. Conversely, both bovine placenta UNC and BNC were functionally closer to human EVT and none of the bovine trophoblast cells resemble human STB. Our analysis suggests that placenta BNC play roles in both invasive and secretory functions to maintain pregnancy in cattle. Clearly, they are using different hormone pathways, as bovine BNC secretes PAGs and PRPs and human STB secretes hCG, which stimulates the corpus luteum to produce progesterone for pregnancy maintenance.[5,58] These differences could be induced during evolution with synepitheliochorial placenta in cattle and the human hemochorial placenta being in direct contact with maternal blood. We recognize that the "end" cells of placental trophoblast differentiation are functionally variable and their relative homologies across different species are not entirely clear. Nonetheless, due to the ethics issues to access human early pregnancies, our molecular and genetic understanding of human placenta trophoblast development, particularly during peri-implantation development is limited, which is a key obstacle to understanding the basis of embryo defects. Therefore, the trophoblast lineage development from this highly informative bovine model will provide valuable information for studying the very earliest stages of human placental development and trophoblast implantation.

Perhaps most importantly, we identified novel markers of cell lineages emerging in the bovine peri-implantation development and the cell-cell interactions that mediate this unique embryo elongation process. While they are largely unexplored, a deeper understanding of their function during these stages might facilitate our understanding of the poorly understood bovine peri-implantation development.

In summary, our work has filled a significant knowledge gap in the study of lineage development over a period of rapid change of embryo elongation and provide foundational information to understanding peri-implantation biology and the causes of early pregnancy failure in the cattle.

Limitations of the study

This study presents the cellular composition and gene expression of bovine peri-implantation lineage development, the function validation of how the identified uncharacterized peri-implantation trophoblast lineage and dynamic transition of the lineage composition during this period is essential for bovine pregnancy establishment and maintenance warrants future studies. Single-cell atlases of human, non-human primates, and other model species during peri-implantation and gastrulation stages have been emerging. However, our analysis narrows to the peri-implantation stages from day 12 to day 18 where embryos can be recovered by standard non-surgical flushing, the lack of more advanced implantation stage embryos limits the scope of our cross-species lineage comparisons giving the diversity of morphology, timing, and length of development, and implantation strategy during this critical period across mammalian species. Finally, the spatial genome-wide sequencing has allowed the direct exploration of the location and dynamics of mRNAs. It has opened up new avenues for understanding peri-implantation development biology and might facilitate the discovery of the molecular causes of the early pregnancy failure during this critical period.

STAR★METHODS

Detailed methods are provided in the online version of this paper and include the following:

- KEY RESOURCES TABLE
- RESOURCE AVAILABILITY
  - Lead contact
  - Materials availability
  - Data and code availability
- EXPERIMENTAL MODEL AND STUDY PARTICIPANT DETAILS
  - Animal care and use
- METHOD DETAILS
  - Cow synchronization protocol
  - Embryos collection
  - Single cell isolation

- Single-cell data pre-processing and clustering
- Constructing trajectory
- Single-cell regulatory network inference and clustering (SCENIC) analysis
- Cell-cell communication analysis
- Immunofluorescent staining
- RNA-FISH analysis

- QUANTIFICATION AND STATISTICAL ANALYSIS

SUPPLEMENTAL INFORMATION

Supplemental information can be found online at https://doi.org/10.1016/j.isci.2024.109605.

ACKNOWLEDGMENTS

We thank Dr. Joel Carter for his assistance with embryo flushing. This work was supported by the NIH Eunice Kennedy Shriver National Institute of Child Health and Human Development (R01HD102533) and USDA National Institute of Food and Agriculture (2019-67016-29863, W4171, Capacity fund hatch project 7004459).

AUTHOR CONTRIBUTIONS

Z.J designed and supervised research. G.S. performed most of the experiments. H.M. performed all genomic data analysis. Y.W. performed single-cell suspension. L.Z., R.I., C.S., E.C., and M.S., helped with embryo collection. K.B. supervised the study. G.S., H.M., and Z.J. interpreted data and assembled the results. G.S., H.M., and Z.J. wrote the articles with inputs from all authors.

DECLARATION OF INTERESTS

The authors declare no competing or financial interests.

Received: July 3, 2023
Revised: March 14, 2024
Accepted: March 25, 2024
Published: March 27, 2024

REFERENCES

1. Inskeep, E.K., and Dailey, R.A. (2005). Embryonic death in cattle. Vet. Clin. North Am. Food Anim. Pract. *21*, 437–461. https://doi.org/10.1016/j.cvfa.2005.02.002.
2. Dunne, L.D., Diskin, M.G., and Sreenan, J.M. (2000). Embryo and foetal loss in beef heifers between day 14 of gestation and full term. Anim. Reprod. Sci. *58*, 39–44. https://doi.org/10.1016/s0378-4320(99)00088-3.
3. Spencer, T.E., Forde, N., and Lonergan, P. (2016). Insights into conceptus elongation and establishment of pregnancy in ruminants. Reprod. Fertil. Dev. *29*, 84–100. https://doi.org/10.1071/RD16359.
4. Wen, J., Zeng, Y., Fang, Z., Gu, J., Ge, L., Tang, F., Qu, Z., Hu, J., Cui, Y., Zhang, K., et al. (2017). Single-cell analysis reveals lineage segregation in early post-implantation mouse embryos. J. Biol. Chem. *292*, 9840–9854. https://doi.org/10.1074/jbc.M117.780585.
5. Argelaguet, R., Clark, S.J., Mohammed, H., Stapel, L.C., Krueger, C., Kapourani, C.A., Imaz-Rosshandler, I., Lohoff, T., Xiang, Y., Hanna, C.W., et al. (2019). Multi-omics profiling of mouse gastrulation at single-cell resolution. Nature *576*, 487–491. https://doi.org/10.1038/s41586-019-1825-8.
6. Zhai, J., Guo, J., Wan, H., Qi, L., Liu, L., Xiao, Z., Yan, L., Schmitz, D.A., Xu, Y., Yu, D., et al. (2022). Primate gastrulation and early organogenesis at single-cell resolution. Nature *612*, 732–738. https://doi.org/10.1038/s41586-022-05526-y.
7. Zhou, F., Wang, R., Yuan, P., Ren, Y., Mao, Y., Li, R., Lian, Y., Li, J., Wen, L., Yan, L., et al. (2019). Reconstituting the transcriptome and DNA methylome landscapes of human implantation. Nature *572*, 660–664. https://doi.org/10.1038/s41586-019-1500-0.
8. West, R.C., Ming, H., Logsdon, D.M., Sun, J., Rajput, S.K., Kile, R.A., Schoolcraft, W.B., Roberts, R.M., Krisher, R.L., Jiang, Z., and Yuan, Y. (2019). Dynamics of trophoblast differentiation in peri-implantation-stage human embryos. Proc. Natl. Acad. Sci. USA *116*, 22635–22644. https://doi.org/10.1073/pnas.1911362116.
9. Bazer, F.W., Spencer, T.E., Johnson, G.A., Burghardt, R.C., and Wu, G. (2009). Comparative aspects of implantation. Reproduction *138*, 195–209. https://doi.org/10.1530/REP-09-0158.
10. Rossant, J. (2011). Developmental biology: A mouse is not a cow. Nature *471*, 457–458. https://doi.org/10.1038/471457a.
11. Jiang, Z., Sun, J., Dong, H., Luo, O., Zheng, X., Obergfell, C., Tang, Y., Bi, J., O'Neill, R., Ruan, Y., et al. (2014). Transcriptional profiles of bovine in vivo pre-implantation development. BMC Genom. *15*, 756. https://doi.org/10.1186/1471-2164-15-756.
12. Daigneault, B.W., Rajput, S., Smith, G.W., and Ross, P.J. (2018). Embryonic POU5F1 is Required for Expanded Bovine Blastocyst Formation. Sci. Rep. *8*, 7753. https://doi.org/10.1038/s41598-018-25964-x.
13. Halstead, M.M., Ma, X., Zhou, C., Schultz, R.M., and Ross, P.J. (2020). Chromatin remodeling in bovine embryos indicates species-specific regulation of genome activation. Nat. Commun. *11*, 4654. https://doi.org/10.1038/s41467-020-18508-3.
14. Davenport, K.M., Ortega, M.S., Liu, H., O'Neil, E.V., Kelleher, A.M., Warren, W.C., and Spencer, T.E. (2023). Single-nuclei RNA sequencing (snRNA-seq) uncovers trophoblast cell types and lineages in the mature bovine placenta. Proc. Natl. Acad. Sci. USA *120*, e2221526120. https://doi.org/10.1073/pnas.2221526120.
15. Galdos-Riveros, A.C., Favaron, P.O., Will, S.E.A.L., Miglino, M.A., and Maria, D.A. (2015). Bovine yolk sac: from morphology to metabolomic and proteomic profiles. Genet. Mol. Res. *14*, 6223–6238. https://doi.org/10.4238/2015.June.9.8.
16. Hue, I. (2016). Determinant molecular markers for peri-gastrulating bovine embryo development. Reprod. Fertil. Dev. *28*, 51–65. https://doi.org/10.1071/RD15355.
17. Negrón-Pérez, V.M., Zhang, Y., and Hansen, P.J. (2017). Single-cell gene expression of the bovine blastocyst. Reproduction *154*, 627–644. https://doi.org/10.1530/REP-17-0345.
18. Wei, Q., Zhong, L., Zhang, S., Mu, H., Xiang, J., Yue, L., Dai, Y., and Han, J. (2017). Bovine lineage specification revealed by single-cell gene expression analysis from zygote to

blastocyst. Biol. Reprod. *97*, 5–17. https://doi.org/10.1093/biolre/iox071.
19. Artus, J., Hue, I., and Acloque, H. (2020). Preimplantation development in ungulates: a 'menage a quatre' scenario. Reproduction *159*, R151–R172. https://doi.org/10.1530/REP-19-0348.
20. Blakeley, P., Fogarty, N.M.E., del Valle, I., Wamaitha, S.E., Hu, T.X., Elder, K., Snell, P., Christie, L., Robson, P., and Niakan, K.K. (2015). Defining the three cell lineages of the human blastocyst by single-cell RNA-seq. Development *142*, 3151–3165. https://doi.org/10.1242/dev.123547.
21. Liu, T., Li, J., Yu, L., Sun, H.X., Li, J., Dong, G., Hu, Y., Li, Y., Shen, Y., Wu, J., and Gu, Y. (2021). Cross-species single-cell transcriptomic analysis reveals pre-gastrulation developmental differences among pigs, monkeys, and humans. Cell Discov. *7*, 8. https://doi.org/10.1038/s41421-020-00238-x.
22. Liu, D., Chen, Y., Ren, Y., Yuan, P., Wang, N., Liu, Q., Yang, C., Yan, Z., Yang, M., Wang, J., et al. (2022). Primary specification of blastocyst trophectoderm by scRNA-seq: New insights into embryo implantation. Sci. Adv. *8*, eabj3725. https://doi.org/10.1126/sciadv.abj3725.
23. van Leeuwen, J., Berg, D.K., and Pfeffer, P.L. (2015). Morphological and Gene Expression Changes in Cattle Embryos from Hatched Blastocyst to Early Gastrulation Stages after Transfer of In Vitro Produced Embryos. PLoS One *10*, e0129787. https://doi.org/10.1371/journal.pone.0129787.
24. Maddox-Hyttel, P., Alexopoulos, N.I., Vajta, G., Lewis, I., Rogers, P., Cann, L., Callesen, H., Tveden-Nyborg, P., and Trounson, A. (2003). Immunohistochemical and ultrastructural characterization of the initial post-hatching development of bovine embryos. Reproduction *125*, 607–623.
25. Hou, J., Charters, A.M., Lee, S.C., Zhao, Y., Wu, M.K., Jones, S.J.M., Marra, M.A., and Hoodless, P.A. (2007). A systematic screen for genes expressed in definitive endoderm by Serial Analysis of Gene Expression (SAGE). BMC Dev. Biol. *7*, 92. https://doi.org/10.1186/1471-213X-7-92.
26. Drukker, M., Tang, C., Ardehali, R., Rinkevich, Y., Seita, J., Lee, A.S., Mosley, A.R., Weissman, I.L., and Soen, Y. (2012). Isolation of primitive endoderm, mesoderm, vascular endothelial and trophoblast progenitors from human pluripotent stem cells. Nat. Biotechnol. *30*, 531–542. https://doi.org/10.1038/nbt.2239.
27. Dubois, N.C., Hofmann, D., Kaloulis, K., Bishop, J.M., and Trumpp, A. (2006). Nestin-Cre transgenic mouse line Nes-Cre1 mediates highly efficient Cre/loxP mediated recombination in the nervous system, kidney, and somite-derived tissues. Genesis *44*, 355–360. https://doi.org/10.1002/dvg.20226.
28. Harvey, N.T., Hughes, J.N., Lonic, A., Yap, C., Long, C., Rathjen, P.D., and Rathjen, J. (2010). Response to BMP4 signalling during ES cell differentiation defines intermediates of the ectoderm lineage. J. Cell Sci. *123*, 1796–1804. https://doi.org/10.1242/jcs.047530.
29. Wolf, E., Arnold, G.J., Bauersachs, S., Beier, H.M., Blum, H., Einspanier, R., Fröhlich, T., Herrler, A., Hiendleder, S., Kölle, S., et al. (2003). Embryo-maternal communication in bovine - strategies for deciphering a complex cross-talk. Reprod. Domest. Anim. *38*, 276–289. https://doi.org/10.1046/j.1439-0531.2003.00435.x.
30. Boroviak, T., Stirparo, G.G., Dietmann, S., Hernando-Herraez, I., Mohammed, H., Reik, W., Smith, A., Sasaki, E., Nichols, J., and Bertone, P. (2018). Single cell transcriptome analysis of human, marmoset and mouse embryos reveals common and divergent features of preimplantation development. Development *145*, dev167833. https://doi.org/10.1242/dev.167833.
31. Roberts, R.M. (2007). Interferon-tau, a Type 1 interferon involved in maternal recognition of pregnancy. Cytokine Growth Factor Rev. *18*, 403–408. https://doi.org/10.1016/j.cytogfr.2007.06.010.
32. Spencer, T.E., Burghardt, R.C., Johnson, G.A., and Bazer, F.W. (2004). Conceptus signals for establishment and maintenance of pregnancy. Anim. Reprod. Sci. *82–83*, 537–550. https://doi.org/10.1016/j.anireprosci.2004.04.014.
33. Spencer, T.E., and Hansen, T.R. (2015). Implantation and Establishment of Pregnancy in Ruminants. Adv. Anat. Embryol. Cell Biol. *216*, 105–135. https://doi.org/10.1007/978-3-319-15856-3_7.
34. Wooding, F.B.P. (2022). The ruminant placental trophoblast binucleate cell: an evolutionary breakthrough. Biol. Reprod. *107*, 705–716. https://doi.org/10.1093/biolre/ioac107.
35. Gerri, C., McCarthy, A., Alanis-Lobato, G., Demtschenko, A., Bruneau, A., Loubersac, S., Fogarty, N.M.E., Hampshire, D., Elder, K., Snell, P., et al. (2020). Initiation of a conserved trophectoderm program in human, cow and mouse embryos. Nature *587*, 443–447. https://doi.org/10.1038/s41586-020-2759-x.
36. Zhang, Z., Wang, Y., Wang, Y., Wang, C., Shuai, Y., Luo, J., and Liu, R. (2021). BCAR3 promotes head and neck cancer growth and is associated with poor prognosis. Cell Death Discov. *7*, 316. https://doi.org/10.1038/s41420-021-00714-7.
37. Bossan, A., Ottman, R., Andl, T., Hasan, M.F., Mahajan, N., Coppola, D., and Chakrabarti, R. (2018). Expression of FGD4 positively correlates with the aggressive phenotype of prostate cancer. BMC Cancer *18*, 1257. https://doi.org/10.1186/s12885-018-5096-9.
38. Zhang, H., Zhu, H., Deng, G., Zito, C.R., Oria, V.O., Rane, C.K., Zhang, S., Weiss, S.A., Tran, T., Adeniran, A., et al. (2020). PLEKHA5 regulates tumor growth in metastatic melanoma. Cancer *126*, 1016–1030. https://doi.org/10.1002/cncr.32611.
39. Davenport, K.M., O'Neil, E.V., Ortega, M.S., Patterson, A., Kelleher, A.M., Warren, W.C., and Spencer, T.E. (2023). Single cell insights into development of the bovine placentadagger. Biol. Reprod. https://doi.org/10.1093/biolre/ioad123.
40. Nowotschin, S., Setty, M., Kuo, Y.Y., Liu, V., Garg, V., Sharma, R., Simon, C.S., Saiz, N., Gardner, R., Boutet, S.C., et al. (2019). The emergent landscape of the mouse gut endoderm at single-cell resolution. Nature *569*, 361–367. https://doi.org/10.1038/s41586-019-1127-1.
41. Xiang, L., Yin, Y., Zheng, Y., Ma, Y., Li, Y., Zhao, Z., Guo, J., Ai, Z., Niu, Y., Duan, K., et al. (2020). A developmental landscape of 3D-cultured human pre-gastrulation embryos. Nature *577*, 537–542. https://doi.org/10.1038/s41586-019-1875-y.
42. Jia, G.X., Ma, W.J., Wu, Z.B., Li, S., Zhang, X.Q., He, Z., Wu, S.X., Tao, H.P., Fang, Y., Song, Y.W., et al. (2023). Single-cell transcriptomic characterization of sheep conceptus elongation and implantation. Cell Rep. *42*, 112860. https://doi.org/10.1016/j.celrep.2023.112860.
43. Nakamura, T., Okamoto, I., Sasaki, K., Yabuta, Y., Iwatani, C., Tsuchiya, H., Seita, Y., Nakamura, S., Yamamoto, T., and Saitou, M. (2016). A developmental coordinate of pluripotency among mice, monkeys and humans. Nature *537*, 57–62. https://doi.org/10.1038/nature19096.
44. Vigneault, C., McGraw, S., Massicotte, L., and Sirard, M.A. (2004). Transcription factor expression patterns in bovine in vitro-derived embryos prior to maternal-zygotic transition. Biol. Reprod. *70*, 1701–1709. https://doi.org/10.1095/biolreprod.103.022970.
45. Bogliotti, Y.S., Chung, N., Paulson, E.E., Chitwood, J., Halstead, M., Kern, C., Schultz, R.M., and Ross, P.J. (2020). Transcript profiling of bovine embryos implicates specific transcription factors in the maternal-to-embryo transition. Biol. Reprod. *102*, 671–679. https://doi.org/10.1093/biolre/ioz209.
46. Paul, S., Home, P., Bhattacharya, B., and Ray, S. (2017). GATA factors: Master regulators of gene expression in trophoblast progenitors. Placenta *60*, S61–S66. https://doi.org/10.1016/j.placenta.2017.05.005.
47. Hashimoto, M., and Sasaki, H. (2019). Epiblast Formation by TEAD-YAP-Dependent Expression of Pluripotency Factors and Competitive Elimination of Unspecified Cells. Dev. Cell *50*, 139–154.e5. https://doi.org/10.1016/j.devcel.2019.05.024.
48. Artus, J., Piliszek, A., and Hadjantonakis, A.K. (2011). The primitive endoderm lineage of the mouse blastocyst: sequential transcription factor activation and regulation of differentiation by Sox17. Dev. Biol. *350*, 393–404. https://doi.org/10.1016/j.ydbio.2010.12.007.
49. Farrugia, A.J., Rodríguez, J., Orgaz, J.L., Lucas, M., Sanz-Moreno, V., and Calvo, F. (2020). CDC42EP5/BORG3 modulates SEPT9 to promote actomyosin function, migration, and invasion. J. Cell Biol. *219*, e201912159. https://doi.org/10.1083/jcb.201912159.
50. Vesque, C., Anselme, I., Couvé, E., Charnay, P., and Schneider-Maunoury, S. (2006). Cloning of vertebrate Protogenin (Prtg) and comparative expression analysis during axis elongation. Dev. Dyn. *235*, 2836–2844. https://doi.org/10.1002/dvdy.20898.
51. Scholler, M., Wadsack, C., Metso, J., Chirackal Manavalan, A.P., Sreckovic, I., Schweinzer, C., Hiden, U., Jauhiainen, M., Desoye, G., and Panzenboeck, U. (2012). Phospholipid transfer protein is differentially expressed in human arterial and venous placental endothelial cells and enhances cholesterol efflux to fetal HDL. J. Clin. Endocrinol. Metab. *97*, 2466–2474. https://doi.org/10.1210/jc.2011-2969.
52. Zhu, M., and Zernicka-Goetz, M. (2020). Principles of Self-Organization of the Mammalian Embryo. Cell *183*, 1467–1478. https://doi.org/10.1016/j.cell.2020.11.003.
53. Agrogiannis, G.D., Sifakis, S., Patsouris, E.S., and Konstantinidou, A.E. (2014). Insulin-like growth factors in embryonic and fetal growth and skeletal development (Review). Mol. Med. Rep. *10*, 579–584. https://doi.org/10.3892/mmr.2014.2258.
54. Yu, L., Wei, Y., Duan, J., Schmitz, D.A., Sakurai, M., Wang, L., Wang, K., Zhao, S., Hon, G.C., and Wu, J. (2021). Blastocyst-like structures generated from human pluripotent stem cells. Nature *591*, 620–626. https://doi.org/10.1038/s41586-021-03356-y.

55. Gough, N.R. (2012). Focus issue: Wnt and beta-catenin signaling in development and disease. Sci. Signal. *5*, eg2. https://doi.org/10.1126/scisignal.2002806.

56. Xu, C., Zhu, S., Wu, M., Han, W., and Yu, Y. (2014). Functional receptors and intracellular signal pathways of midkine (MK) and pleiotrophin (PTN). Biol. Pharm. Bull. *37*, 511–520. https://doi.org/10.1248/bpb.b13-00845.

57. Pijuan-Sala, B., Griffiths, J.A., Guibentif, C., Hiscock, T.W., Jawaid, W., Calero-Nieto, F.J., Mulas, C., Ibarra-Soria, X., Tyser, R.C.V., Ho, D.L.L., et al. (2019). A single-cell molecular map of mouse gastrulation and early organogenesis. Nature *566*, 490–495. https://doi.org/10.1038/s41586-019-0933-9.

58. Memili, E., and First, N.L. (1998). Developmental changes in RNA polymerase II in bovine oocytes, early embryos, and effect of alpha-amanitin on embryo development. Mol. Reprod. Dev. *51*, 381–389. https://doi.org/10.1002/(SICI)1098-2795(199812)51:4<381::AID-MRD4>3.0.CO;2-G.

59. Wolock, S.L., Lopez, R., and Klein, A.M. (2019). Scrublet: Computational Identification of Cell Doublets in Single-Cell Transcriptomic Data. Cell Syst. *8*, 281–291.e9. https://doi.org/10.1016/j.cels.2018.11.005.

60. Satija, R., Farrell, J.A., Gennert, D., Schier, A.F., and Regev, A. (2015). Spatial reconstruction of single-cell gene expression data. Nat. Biotechnol. *33*, 495–502. https://doi.org/10.1038/nbt.3192.

61. Yu, G., Wang, L.G., Han, Y., and He, Q.Y. (2012). clusterProfiler: an R package for comparing biological themes among gene clusters. OMICS *16*, 284–287. https://doi.org/10.1089/omi.2011.0118.

62. Qiu, X., Mao, Q., Tang, Y., Wang, L., Chawla, R., Pliner, H.A., and Trapnell, C. (2017). Reversed graph embedding resolves complex single-cell trajectories. Nat. Methods *14*, 979–982. https://doi.org/10.1038/nmeth.4402.

63. Trapnell, C., Cacchiarelli, D., Grimsby, J., Pokharel, P., Li, S., Morse, M., Lennon, N.J., Livak, K.J., Mikkelsen, T.S., and Rinn, J.L. (2014). The dynamics and regulators of cell fate decisions are revealed by pseudotemporal ordering of single cells. Nat. Biotechnol. *32*, 381–386. https://doi.org/10.1038/nbt.2859.

64. Jin, S., Guerrero-Juarez, C.F., Zhang, L., Chang, I., Ramos, R., Kuan, C.H., Myung, P., Plikus, M.V., and Nie, Q. (2021). Inference and analysis of cell-cell communication using CellChat. Nat. Commun. *12*, 1088. https://doi.org/10.1038/s41467-021-21246-9.

65. Aibar, S., González-Blas, C.B., Moerman, T., Huynh-Thu, V.A., Imrichova, H., Hulselmans, G., Rambow, F., Marine, J.C., Geurts, P., Aerts, J., et al. (2017). SCENIC: single-cell regulatory network inference and clustering. Nat. Methods *14*, 1083–1086. https://doi.org/10.1038/nmeth.4463.

66. Korsunsky, I., Millard, N., Fan, J., Slowikowski, K., Zhang, F., Wei, K., Baglaenko, Y., Brenner, M., Loh, P.R., and Raychaudhuri, S. (2019). Fast, sensitive and accurate integration of single-cell data with Harmony. Nat. Methods *16*, 1289–1296. https://doi.org/10.1038/s41592-019-0619-0.

STAR★METHODS

KEY RESOURCES TABLE

REAGENT or RESOURCE	SOURCE	IDENTIFIER
Antibodies		
Anti-PTGS2	Sigma	Cat# SAB2500267; RRID: AB_10603695
Alexa Fluor 488 anti-goat antibody	Invitrogen	Cat# A32814; RRID: AB_2762838
Phalloidin-iFluor 488	Abcam	Cat# ab176753; RRID: not available
Anti-KRT8	Origene	Cat# BP5075; RRID: not available
Anti-SOX17	R&D systems	Cat# AF1924; RRID: not available
Anti-Vimectin	Invitrogen	Cat# MA5-11883; RRID: not available
Biological samples		
Bovine embryos day 12,14,16,18	RBC – Louisiana State University	N/A
Chemicals, peptides, and recombinant proteins		
TrypLE Express enzyme (1X)	Gibco	Car# 12605-010
Dulbecco's Phosphate Buffered Saline	Sigma	Cat# D8537
Fetal Bovine Serum	Gibco	Cat# 16000044
Bovine Serum Albumin	MP Bio	Cat# 0219989925
Controlled Internal Drug Release (CIDR)	Zoetis	Reg. No. G1916
Fertagyl (Gonadorelin)	Merck Animal Health	NDC 57926-477
Folltropin (Follicle-Stimulating Hormone)	Vetoquinol	NDC 17030-102-70
Lutalyse (Dinoprost Tromethamine Injection)	Zoetis	NDC 54771-1327
Critical commercial assays		
Chromium Next GEM Single Cel 3′ Reagent Kit v3.1 Dual Index	10x Genomics	Cat# 1000268
ViewRNA-ISH cell assay kit	Thermo Fisher	Cat# QVC0001
ViewRNA-ISH cell 740 Module	Thermo Fisher	Cat#QVC0200
Deposited data		
Bovine scRNA-seq data from this paper	This paper	GSE234335
Bovine scRNA-seq data from day 17–50	Davenport et al.[14,39]	GSE234524
Bovine sc RNA-seq data from day 195	Davenport et al.[14,39]	GSE214407
Mouse scRNA-seq data from 4.5 dpf embryos	Nowotschin et al.[40]	GSE123046
Sheep scRNA-seq data from 12, 16, 19 dpf embryos	Jia et al.[42]	BioProject PRJNA987334
Human scRNA-seq data from 3D-cultured human pre-gastrulation embryos	Xiang et al.[41]	GSE136447
Monkey scRNA-seq data from 8 to 14 dpf embryos	Nakamura et al.[43]	GSE74767
Oligonucleotides		
GAPDH probe	Thermo Fisher	Cat# VX-01; assay ID: VF10-4027399-VC
ASCL2 probe	Thermo Fisher	Cat# VX-01; assay ID: VF4-4034455-VC
HAND1 probe	Thermo Fisher	Cat# VX-01; assay ID: VF1-4038876-VC
FADS1 probe	Thermo Fisher	Cat# CVX-01; assay ID: VPPRJ9H
TMEM86A probe	Thermo Fisher	Cat# VX-01; assay ID: VF6-4032746-VC
CTSV probe	Thermo Fisher	Cat# VX-01; assay ID: VF10-4027476-VC
RAPGEF2 probe	Thermo Fisher	Cat# VX-01; assay ID: VF1-4033190-VC

(*Continued on next page*)

Continued

REAGENT or RESOURCE	SOURCE	IDENTIFIER
Software and algorithms		
CellRanger (v.7.1.0)	10x Genomics	https://support.10xgenomics.com/single-cell-gene-pression/software/pipelines/latest/what-is-cell-ranger
Scrublet (v.0.2.3)	Wolock et al.[59]	https://github.com/allonkleinlab/scrublet
Seurat (v.4.3.0)	Satija et al.[60]	https://github.com/satijalab/seurat
SCP (v.0.4.0)	N/A	https://github.com/zhanghao-njmu/SCP
clusterProfiler (v.4.6.1)	Yu et al.[61]	https://bioconductor.org/packages/release/bioc/html/clusterProfiler.html
Monocle 2 (v.2.26.0)	Qiu et al.[62]	http://cole-trapnell-lab.github.io/monocle-release/docs/
Monocle 3 (v.1.3.1)	Trapnell et al.[63]	https://cole-trapnell-lab.github.io/monocle3/
CellChat (v.1.6.1)	Jin et al.[64]	https://github.com/sqjin/CellChat
SCENIC R (v.1.3.1)	Aibar et al.[65]	https://github.com/aertslab/SCENIC

RESOURCE AVAILABILITY

Lead contact

Further information for resources and reagents should be directed to the lead contact, Zongliang Jiang (z.jiang1@ufl.edu).

Materials availability

This study did not generate new unique reagents.

Data and code availability

- The raw FASTQ files and normalized read accounts per gene are available at Gene Expression Omnibus (GEO) (https://www.ncbi.nlm.nih.gov/geo/) under the accession number GSE234335. This paper analyzes publicly available data. The accession numbers for the datasets are listed in the key resources table.
- This paper does not report original code.
- Any additional information required to reanalyze the data reported in this paper is available from the lead contact upon request.

EXPERIMENTAL MODEL AND STUDY PARTICIPANT DETAILS

Animal care and use

Bovine peri-implantation embryos were collected from non-lactating, 3-year-old crossbreed (Bos taurus x Bos indicus) cows. The experiments were conducted under animal use protocols (A2021-21) and (202300000191) approved by the Institutional Animal Care and Use Committee of the Louisiana State University Agricultural Center and the University of Florida, respectively. All cows were housed in open pasture, and under constant care of the farm staff.

METHOD DETAILS

Cow synchronization protocol

Cows were synchronized starting on day 0 with dominant follicle removal (DFR) followed by insertion of standard 7-day vaginal controlled internal drug release of progesterone (CIDR, Zoetis). On day 2, ovulation-inducing gonadotropin-release hormone (GnRH, Fertagyl, Merk Animal Health) was administered 2 mL intramuscular (IM) injection dose. From day 4–7, follicle-stimulating hormone (FSH, Folltropin, Vetoquinol) was administered twice a day in a decreasing dose (day 4: 1.6 mL, day 5: 1.2 mL, day 6: 1 mL, day 7: 0.8 mL, total dosage 400 UI). Upon CIDR removal on day 7, a dose (5 mL) of prostaglandin (Lutalyse, Zoetis) was administered in the morning and again in the afternoon. 48 h after CIDR removal another 2 mL dose of GnRH was administered via IM injection and artificial insemination was procedure twice in a 12-h interval.

Embryos collection

Bovine peri-implantation embryos were collected 12, 14, 16 18 days after artificial insemination. Embryos were recovered by standard non-surgical flush with lactated ringer solution supplemented with 1% fetal bovine serum and washed with PBS before processing for single cell isolation. All cows were treated with prostaglandin (Lutalyse, Zoetis) after flushing.

Single cell isolation

After embryo collection, fresh embryos were washed with PBS and placed in a 3% FBS in ice-cold PBS. Embryos were centrifuged for 5 min at 400 × g at 4°C. After supernatant aspiration, embryos were resuspended in 200 μL of TrypLE and minced by scissors. 500 μL of TrypLE were added and then embryos were incubated at 37°C in a shaker at 150 rpm for 4–7 min depending on size of embryos. Samples were pipetted every 2 min to avoid large clumps. Dissociation was stopped with same volume of 3% FBS (700 μL), and the suspensions were pass through 70 μm cell strainer and centrifuged for 5 min at 400xg at 4°C. The cell pellet was resuspended with 0.04% BSA in PBS (volume depended on the size of cell pellet). Cell suspensions were filtered through a 40 μm cell strainer into a new 1.5mL Eppendorf tube. Cell viability and concentration were measured using a Countess Automated Cell Counter. The cells with viability at least 80% were proceeded with the 10x Genomics Single Cell Protocol with a target of 10,000 cells per sample. Single cell libraries were prepared using 10x Chromium Next GEM Single Cel 3′ Reagent Kit v3.1 Dual Index following the manufacturer's instructions. Libraries were sequenced with an Illumina Novaseq 6000 System (Novogene).

Single-cell data pre-processing and clustering

To analyze 10X Genomics single-cell data, the base call files (BCL) were transferred to FASTQ files by using CellRanger (v.7.1.0) mkfastq with default parameters, followed by aligning to the most recent bovine reference genome downloaded from Ensembl database (UCD1.2.109), then the doublets were detected and removed from single cells by using Scrublet (0.2.3) with default parameters. The generated count matrices from all the samples were integrated by R package Seurat (4.3.0) utilizing canonical correlation analysis (CCA) with default parameters (https://satijalab.org/seurat/articles/get_started.html).[60] Particularly, in analysis of bovine trophoblast subpopulations from D12 to D195, trophoblast cells from different datasets were integrated with Harmony v1.1.0.[66] The data was scaled for linear dimension reduction and non-linear reduction using principal component analysis (PCA) and UMAP, respectively. The following clustering and visualization were performed by using the Seurat standard workflow with the parameters "dim = 1:30" in "FindNeighbors" function and "resolution = 0.2" in "FindClusters" function. The function "FindAllMarkers" in Seurat was used to identify differentially expressed genes in each defined cluster. The cutoff value to define the differentially expressed genes was p.adjust value <0.05, and fold change >0.25. The UMAP plots and bubble plots with marker genes were generated using "CellDimPlot" and "GroupHeatmap" functions in R package SCP (0.4.0) (https://github.com/zhanghao-njmu/SCP), respectively. Gene ontology (GO) and pathway analysis was performed using R package clusterProfiler (4.6.1), and the GO terms were presented by "dotplot" function in Seurat.

Constructing trajectory

Cell differentiation was inferred for trophoblast subtypes from peri-implantation embryos and from cotyledon part in Day195 of gestation using the Monocle 2 method (2.26.0) with default parameters.[62] Because of the large amount of cell numbers, 1000 cells were randomly selected from each cluster and used for the following analysis. Integrated gene expression matrices with the smaller sample size from each subtype were exported into Monocle by constructing a CellDataSet. Genes detected in less than 20 cells were removed and then the variable genes were defined by "differentialGeneTest" function, the top 1000 genes were used for cell ordering with the "setOrderingFilter" function. Dimensionality reduction was performed using the "DDRTree" reduction method in the reduceDimension step. The root of the pseudotime trajectory was assigned based on the time point of the development (clusters enriched at D12 were considered as root). Pseudotime related genes were defined by using "differentialGeneTest" function. Monocle 3 (1.3.1) was also used to construct the pseudotime trajectory from elongation embryos to D195 cotyledon cells with the default workflow steps (https://cole-trapnell-lab.github.io/monocle3/).[63]

Single-cell regulatory network inference and clustering (SCENIC) analysis

We explored the transcription factor network inference by using the SCENIC R package (version 1.3.1, with the dependent packages RcisTarget 1.17.0, AUCell 1.20.1, and GENIE3 1.20.0).[65] Activity of the regulatory networks was evaluated by the standard workflow by using "runSCENIC_1_coexNetwork2modules", "runSCENIC_2_createRegulons", "runSCENIC_3_scoreCells", and "runSCENIC_4_aucell_binarize" in a row. Then potential direct-binding targets (regulons) were explored based on motif analysis. Next, based on the AUCell algorithm, SCENIC calculates each regulator's activity and builds gene-expression rankings for each cell. To find the main transcription factors regulating bovine peri-implantation embryo development, the regulon activity was averaged. A regulon-group heatmap was generated with pheatmap package in R.

Cell-cell communication analysis

Potential cell–cell interactions based on the expression of known ligand–receptor pairs between different clusters were identified using CellChat (1.6.1).[64] Integrated gene expression matrices from all subtypes were exported from Seurat into CellChat by using "createCellChat" function, followed by preprocessing workflow steps including "identifyOverExpressedGenes", "identifyOverExpressedInteractions", and "projectData" functions with default parameters. The cell-cell communication was then calculated with functions "computeCommunProb", "filterCommunication", "computeCommunProbPathway", and "aggregateNet" in a row with default parameters. The significant intercellular signaling interactions for specific pathway families of molecules were performed with "netVisual" function. To determine the senders and receivers for specific pathways, the function netAnalysis_computeCentrality was applied on the netP data slot. The contribution of each cell

subtype to enriched interaction pathways including both outgoing pattern and incoming pattern were visualized by using netAnalysis_signalingRole_heatmap function.

Immunofluorescent staining

Embryos were fixed with 4% paraformaldehyde (PFA) in 1x DPBS with 0.1% PVA for 20 min at room temperature, washed 3 times in wash buffer (0.1% Triton X-100, 5% BSA in 1xDPBS) for 5 min and permeabilized with 0.1–1% Triton X-100 in PBS for 30 min. After that, embryos were blocked with blocking buffer (PBS containing 5% Donkey serum, 5% BSA, and 0.1% Triton X-100) at room temperature for 1 h. Primary antibodies were diluted in blocking buffer (1:100 dilution) and embryos were incubated in primary antibodies overnight at 4 C. Samples were washed five times for 5 min with wash buffer, and incubated with fluorescent-dye conjugated secondary antibodies (AF-488, AF-555 or AF-647, Invitrogen) diluted in blocking buffer (1:200 dilution) for 2 h at room temperature. Embryos were washed five times with washing buffer. To finalize, embryos were counter-stained with (DAPI) solution at room temperature for 15 min. Phalloidin was directly stained along with the secondary antibodies in the blocking buffer.

RNA-FISH analysis

Fresh embryos were fixed in 4% paraformaldehyde in PBS for 30 min, washed 3 times in PBS and processed using the ViewRNA-ISH cell assay kit following the manufacturer's instructions. Briefly, embryos were passed through protease digestion (dilution 1:4000) for 10 min at room temperature. Then, the embryos were washed with PBS for 5 min, 5 times and transferred to working probe set solution (Probe used in this experiment are listed in star protocol) and incubated for 3 h at 40°C. After hybridization, samples were washed in wash buffer +0.1% Triton X100, and followed sequential steps of pre-amplifier DNA, amplifier DNA and label probes (all processes were performed at 40°C for 30 min and washed with PBS for 5 min, 5 times following each step). Finally, the embryos were transferred to slides and mounted with DAPI prolong gold antifade reagent and covered with coverslips. The images were captured under 20× objective lens Leica Stellaris 8 spectral confocal microscope.

QUANTIFICATION AND STATISTICAL ANALYSIS

Statistical differences between pairs of datasets were analyzed by two-tailed unpaired t-tests. Values of $p < 0.05$ were considered statistically significant. Where applicable, all quantitative data are presented as the mean ± SD. Repeated number was indicated as "n" in figure legends.

Statistical analyses of sequencing data were performed in R. The number for each dataset is defined in the figure legends and text. The generated count matrices from all the samples were integrated by R package Seurat (4.3.0) utilizing canonical correlation analysis (CCA) with default parameters (https://satijalab.org/seurat/articles/get_started.html) and for identifying DEGs between different cell types or different timepoints. Genes with $|\log2\text{fold change}| \geq 1$ and adjusted p value < 0.05 were identified as significant DEGs. Gene ontology (GO) and pathway analysis was performed using R package clusterProfiler (4.6.1). The value of p value < 0.05 was considered significant.